https://e-space.mmu.ac.uk

Use of screen-printed electrodes modified by Prussian blue and analogues in sensing of cysteine

Juliano A. Bonacin[a*], Vera Katic[a], Pãmyla L. dos Santos[a], Christopher W. Foster[b], Craig E. Banks[b*]

[a]Institute of Chemistry, University of Campinas, P. O. Box 6154, 13083-970, Campinas, SP, Brazil

Web: http://bonacin.iqm.unicamp.br Fax: +55 19 3521 3023; Tel: +55 19 3521 3103;

*e-mail:*jbonacin@iqm.unicamp.br*

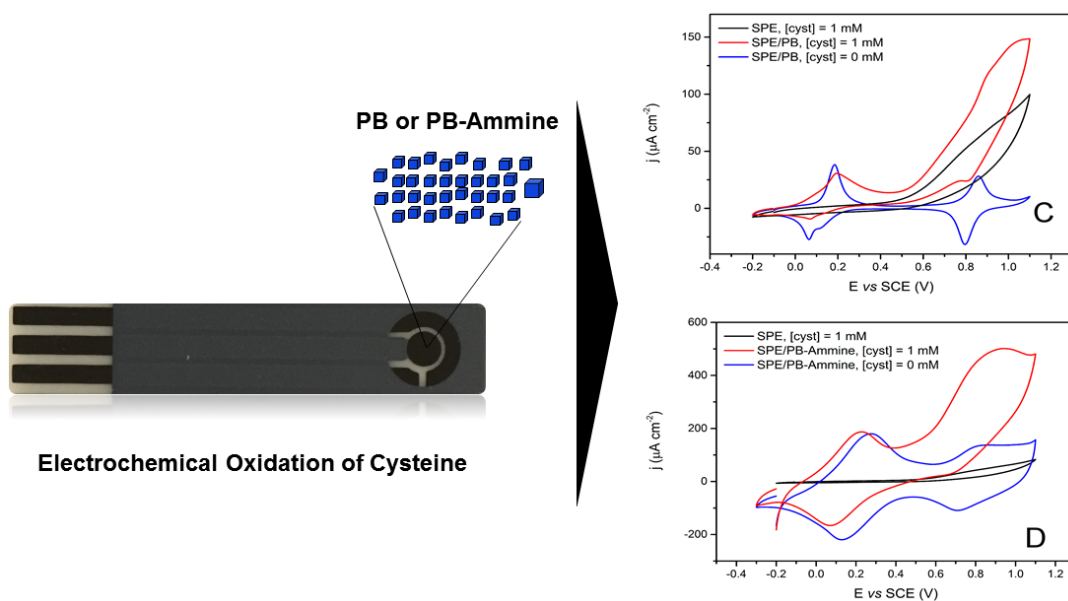[b] Faculty of Science and Engineering, Manchester Metropolitan University, Chester Street, Manchester M15 GD, UK.

Web: http://www.craigbanksresearch.com Fax: +44 (0)1612476831; Tel: +44 (0)1612471196;

*e-mail:*c.banks@mmu.ac.uk

Graphical Abstract

1

2   **Abstract**

3   The utilisation of screen-printing technology allows for a mass scalable approach to producing

4   electrochemical screen-printed electrodes (SPEs) and the presence of a redox mediator can add new

5   possibilities to the electrochemical properties of the SPEs. Among the materials used as redox mediators,

6   cyanidoferrates polymers can be used for electro-oxidation of cysteine. In this work, different monomers

7    $[Fe(CN)_6]^{4-}$ and $[Fe(CN)_5NH_3]^{3-}$ were used to produce Prussian blue (PB) and Prussian blue-Ammine

8   (PB-Ammine), respectively. In addition, two modification methods were compared, the drop-casting

9   and the incorporation of these materials into a *printable ink* were both used. The SPE modified by PB-

10   Ammine (drop-casting) has the highest electroactive area and the highest heterogeneous rate constants

11   are found in SPE modified by PB-Ammine incorporated into the ink. The highest value of the constant

12   of electro-oxidation of cysteine and lowest limit of detection was observed in the SPE modified by PB

13   incorporated into the ink. The studies suggest that the electrocatalytic properties of SPE modified by PB

14   and PB-Ammine are dependents of the availability of Fe^{3+} catalytic sites and the faster chemical reaction

15   between the catalytic sites and the analyte.

16

17

18

1. Introduction

The development of screen-printed electrodes (SPEs) has become a revolution in the world of electrochemical sensors[1,2]. SPEs are planar devices, based upon multiple layers of printable inks that simplify the electroanalytical procedure. Such electrodes allow laboratory analyses to be performed on-site and are suitable for working with microvolumes and decentralized assays [3–5]. Furthermore, the ability to mass produce these screen-printed electrodes reproducibly allows their use as one-shot sensors, alleviating potential memory effects and contamination whilst eradicating the requirement of electrode pretreatment and preparation (electrode polishing, potential cycling *etc*.), as is often the case for conventional solid electrodes (such as glassy carbon, boron-doped diamond and *etc*.)[6–8].

SPEs have been widely used in clinical, environmental, biological, food safety and industrial analysis. The variety of commercials SPEs are available with an array of characteristics (*i.e.* different inks, substrates and heat curing temperatures) that directly influence on their electrochemical behavior[3,5,6]. Typically, carbon materials used as the screen-printed mediators are widely applied within electrochemical research for the determination of biological analytes such as NADH, dopamine or cysteine. In this sense, the analysis of the level of cysteine in the blood may reveal its deficiency and consequently be associated with the slow growth of children, some types of edemas, skin lesions, lethargy, liver damage, diabetes and mainly leukemia, Alzheimer and Parkinson's diseases[9,10].

The electroactive layer is the key to the transduction process in the electrochemical sensing of molecular targets. Due to this, the electroactive coordination polymers (ECP) prepared from cyanidoferrates(II) deserve attention owing to the well-defined chemical behavior, stability of the film, facility in the preparation and wide range of application. In addition, the modulation of the electrochemical processes can be easily achieved by the strategic replacement of ligands in the complex and consequently, the properties are transferred to the ECP[11,12].

Prussian blue is a classic example of an ECP that can have its electrochemical behavior modulated according to the starting complex. For example, ECP or Prussian blue analogous (Prussian

1   blue-Ammine) produced from $[Fe(CN)_5(NH_3)]^{3-}$ have a shift of the electrochemical process Fe^{2+}/Fe^{3+} to

2   Fe^{3+}/Fe^{3+} to lower value when compared with the same process in the Prussian blue. The shift observed

3   is caused by lowering of energy levels of the HOMO orbital of the complex that is influenced by the

4   sigma-donor character of NH_3 as ligand in the iron complex[12,13]. This modulation can be essential for

5   the design of new types of sensors.

6   In this paper, we report the electrochemical behavior of a SPE modified with Prussian blue and

7   Prussian blue-Ammine produced from $[Fe(CN)_5NH_3]^{3-}$ towards the sensing of cysteine. In addition, we

8   compare the characteristics of SPEs with the electroactive materials incorporated within the ink and

9   drop-cast upon the electrode.

10   **2. Experimental**

11   *2.1. Chemicals*

12   Sodium nitroprusside ($Na_2[Fe(CN)_5NO].2H_2O$) was purchased from Acros Organics. Iron(III)

13   chloride, hydrochloric acid (HCl, 36.5-38%), potassium chloride (KCl), acetic acid (CH_3CO_2H, 99.7%)

14   and sodium acetate (CH_3CO_2Na) were purchased from Synth. Sodium iodide (NaI) and ethanol

15   (CH_3CH_2OH) were purchase from Merck. Ammonium hydroxide (NH_4OH, 28% m/v) and L-cysteine

16   hydrochloride ($HSCH_2CH(NH_2)COOH.HCl$) were purchased from Sigma-Aldrich. All chemicals were

17   of analytical grade and used without any further purification and the aqueous solutions were prepared

18   with ultrapure water (>18MΩ cm) obtained from a Milli-Q Plus system (Millipore).

19   *2.2. Synthesis of Na₃[Fe(CN)₅NH₃].3H₂O*

20   Sodium amminepentacyanidoferrate(II) was prepared by addition of 6.0 g of sodium nitroprusside

21   in 40 mL of ammonium hydroxide in an Erlenmeyer. The mixture was stirred until the complete

22   solubilization of $Na_2[Fe(CN)_5NO].2H_2O$. The Erlenmeyer was covered with aluminium foil and the top

23   of the flask covered with cotton to allow the gas to exit. The solution was kept at room temperature,

24   without stirring and in the dark for 3h, turning into dark yellow. Then, 6.0 g of NaI was added for

1   precipitation of a yellow solid. Finally, ethanol was slowly added to complete precipitation of the solid.

2   The final product was filtered, washed with ethanol and dried under vacuum until constant weight. Yield:

3   87%. Elemental analysis calculated for $C_5H_9FeN_6Na_3O_3$ (325.98 g mol^{-1}): C 18.42%, H 2.78%, N

4   25.78%. Found: C 18.51%, H 2.69% and N 25.37%.

5   *2.3.Synthesis of the ferric cyanidoferrates polymers*

6   Ferric hexacyanidoferrate(II), known as Prussian blue (PB) and ferric pentacyanidoferrate(II) (PB-

7   Ammine) were prepared by chemical method. It consists in adding $FeCl_3$ in excess (4.10^{-2} mol L^{-1}) to a

8   solution of potassium hexacyanidoferrate or sodium amminepentacyanidoferrate (1.10^{-2} mol L^{-1}) under

9   stirring. After 15 minutes, PB or PB-Ammine was precipitated in acetone and it was isolated by

10   centrifugation.

11   *2.4.Modification of the electrodes*

12   The bare screen-printed electrodes (SPEs) were fabricated as described previously[14,15]. The

13   modified SPEs by ECP were prepared by two different methods. Firstly, 5.0 µL of suspensions of PB

14   (2.0 mg mL^{-1}) and PB-Ammine (2.0 mg mL^{-1}) were drop-casted upon the surfaces of SPEs, which were

15   subsequently left to dry overnight under vacuum at room temperature. The modified electrodes produced

16   by the drop-casting method were labeled SPE/PB and SPE/PB-Ammine. Secondly, 10% (m/m) of PB

17   and PB-Ammine were incorporated into the carbon-graphite ink (product code C2000802P2; Gwent

18   Electronic Materials Ltd., U.K.) and used in the same printing process of the bare SPEs. The modified

19   SPEs fabricated *via* the second method were labeled PB-SPE and PB-Ammine-SPE. After the

20   modification, the SPEs were activated by applying 25 voltammetric cycles from -0.2 V to 0.6 V *vs* SCE

21   in a solution of HCl 0.1 mol L^{-1} containing KCl 0.1 mol L^{-1} at a scan rate of 50 mV s^{-1}. Afterwards, the

22   electrodes were dried in an oven at 60°C for 1 hour.

1 *2.5.Electrochemical measurements*

2   Cyclic voltammetry (CV) measurements of SPE/PB and SPE/PB-Ammine were carried out using

3 a Palmsens Emstat (Palmsens, Netherlands) potentiostat. CV of PB-SPE and PB-Ammine-SPE were

4 performed on an AUTOLAB modular electrochemical system (ECO Chemie, Utrecht, Netherlands)

5 equipped with a STAT 12 module and driven by NOVA 2.1 software. The bare or modified SPE were

6 used as working electrode, a saturated calomel electrode (SCE) as reference electrode, and a platinum

7 wire as auxiliary electrode. Acetate buffer (ABS, pH=6) containing KCl and HCl/KCl (pH=1) solutions

8 were used for the stability measurements. Oxygen was removed by bubbling nitrogen for approximately

9 10 min through the solution before each electrochemical measurement.

10   The electroactive areas of the SPEs were determined *via* cyclic voltammetry in 1.0 mmol L^{-1} of

11 $[Ru(NH_3)_6]^{3+}$ and 0.1 mol L^{-1} KCl at different scan rates, according to the Randles-Ševčíck equation

12 (Eq.1):

13
$$i_p = 2.69 \times 10^5 \, n^{\frac{3}{2}} A D^{\frac{1}{2}} C v^{\frac{1}{2}} \qquad (1)$$

14   The heterogeneous rate constants of the SPEs, k^0, were presented determined using the Nicholson

15 method by the following equation (Eq.2):

16
$$k^0 = \left[2.18 \left(\frac{D \propto nFv}{RT} \right)^{\frac{1}{2}} \right] exp \left[- \left(\frac{\propto^2 nF}{RT} \right) \Delta E_P \right] \qquad (2)$$

17 were i_p is the peak current, n is the number of electrons transferred in the electrochemical process, A is

18 electrode area, D is the diffusion coefficient (9.10 x 10^{-6} cm^2 s^{-1} for $[Ru(NH_3)_6]^{3+}$), C is the redox probe

19 concentration and v is the applied voltammetric scan rate, R the gas constant, and T the temperature of

20 the solution, $\propto$ is assumed to correspond to 0.5, ΔE_P is peak-to-peak separation[4,16] .

1 *2.6.Cysteine detection*

2   Electrochemical detection of cysteine was carried out in the same conventional three-electrode

3 electrochemical cell. Chronoamperometry measurements were performed at applied potential of 0.8 V

4 *vs.* SCE, upon successive additions of 0.1 mol L^{-1} L-cysteine hydrochloride stock solution, under N_2

5 atmosphere. Acetate buffer solution (0.1M, pH=6.0) containing 0.1 M KCl was used as supporting

6 electrolyte.

7

8 **3.   Results and Discussion**

9 *3.1.Electrochemical properties of the screen-printed electrodes*

15   The electrochemical behavior of the bare and modified SPEs was investigated by cyclic

16 voltammetry and is depicted within Figure 1. The bare SPE does not exhibit any redox peaks. After 30

17 voltammetric cycles (Fig. S1), the capacitive current increases, probably due to the alterations in the

18 surface area and roughness of the electrodes. Functional groups, impurities, defects and edge plane-like

19 sites on the graphite present in the ink also contribute to alterations within the double-layer
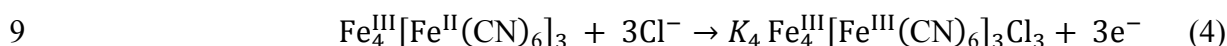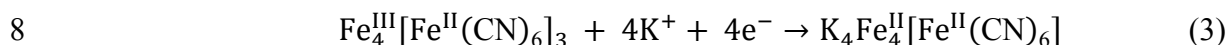
20 capacitance[17,18].

21
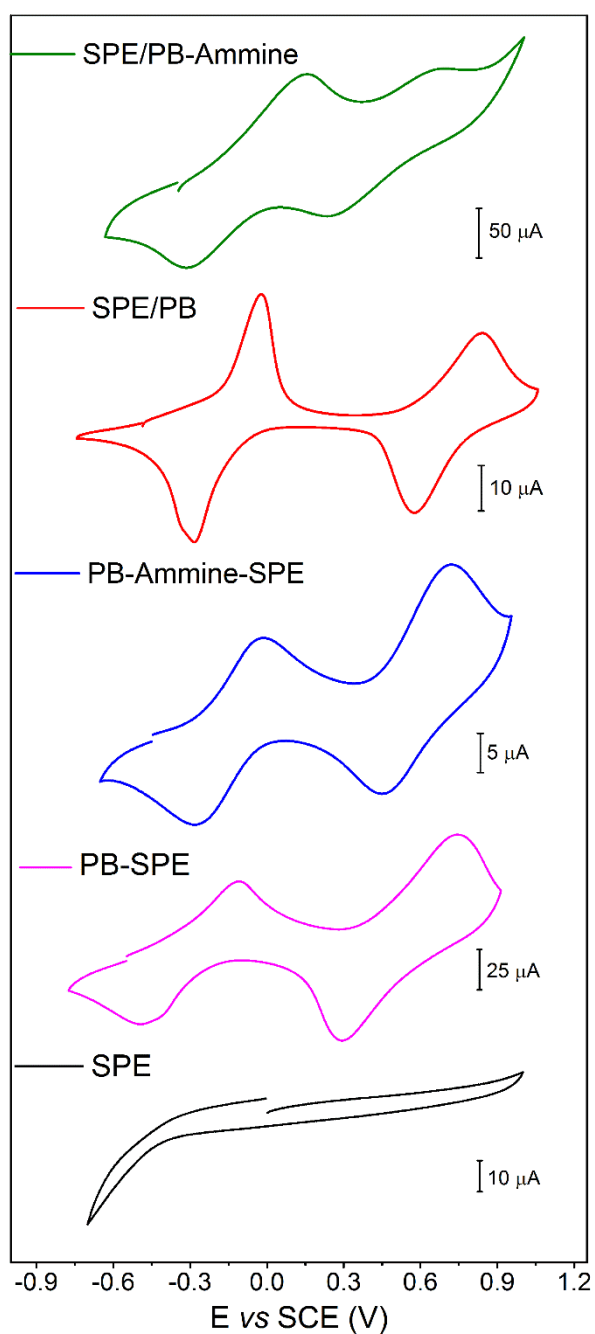
Figure 1: Comparison between the cyclic voltammograms of the bare SPE and modified: PB-SPE, PB-Ammine-SPE, SPE/PB and SPE/PB-Ammine in 0.1 M ABS (pH = 6.0) and 0.1 M KCl at 50 mV s^{-1}.

All the modified SPEs exhibit two well-defined pairs of redox peaks ~ + 0.12 and + 0.80 V *vs.* SCE, which are ascribed to the electrochemical process between Prussian white (PW) to PB (Fe^{2+}/Fe^{2+} → Fe^{2+}/Fe^{3+}), and PB to Belin green (BG, Fe^{2+}/Fe^{3+} → Fe^{3+}/Fe^{3+}), respectively. The composition of the

modified SPEs is associated with the "insoluble" form of the ferric cyanidoferrate, synthesized from excess of Fe^{3+}. The "insoluble" form can be converted to the "soluble" after performing cyclic voltammetry experiments in KCl, because of the insertion of K^+ in the interstitial sites of the PB[19]. The reduction and oxidation reactions of "soluble" (Eq. 1 and 2) and "insoluble" forms of PB (Eq. 3 and 4) as described as follow[20]:

$$KFe^{III}[Fe^{II}(CN)_6] + K^+ + e^- \rightarrow K_2Fe^{II}[Fe^{II}(CN)_6] \qquad (1)$$

$$KFe^{III}[Fe^{II}(CN)_6] \rightarrow K_2Fe^{II}[Fe^{II}(CN)_6] + K^+ + e^- \qquad (2)$$

$$Fe_4^{III}[Fe^{II}(CN)_6]_3 + 4K^+ + 4e^- \rightarrow K_4Fe_4^{II}[Fe^{II}(CN)_6] \qquad (3)$$

$$Fe_4^{III}[Fe^{II}(CN)_6]_3 + 3Cl^- \rightarrow K_4\,Fe_4^{III}[Fe^{III}(CN)_6]_3Cl_3 + 3e^- \qquad (4)$$
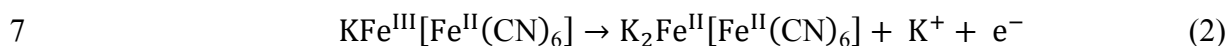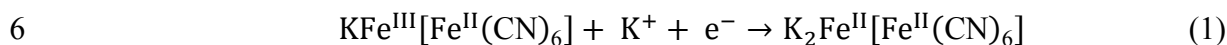
As described by the Eq. 1-4, the electrochemical process of Prussian blue is mediated by the transport of K^+ and Cl^- into and out of the film to maintain the electroneutrality. Thus, the redox processes of the modified electrodes are not surface-confined and depend on the diffusion of the ions into the structure of the materials. This is confirmed by the non-linear correlation between the peak current and the scan rates, as presented in Figures S.2-S.5.

The formal potential values of these processes ($E_{1/2}$) at the modified electrodes are presented in Tables S7-S8. The lowest values of $E_{1/2}$ of the SPE modified with PB-Ammine reflects the weaker π-acceptance character of the NH_3 ligand when compared with CN^-, consequently Fe^{3+} has a higher charge density facilitating the oxidation of this metal[13].

To study the electron transfer properties and determine the electroactive areas (A_e) of the bare and modified SPEs, cyclic voltammetry was carried out in the presence of the outer-sphere redox probe hexaammineruthenium(III) in 0.1 M KCl, Figure S.6.

The electroactive areas of the PB or electroactive coordination polymers can be modulated by the utilisation of different monomers. Recently, an improvement of the A_e of the PB produced from pentacyanidoferrate complexes by drop-casting and potentiostatic methods was reported[11,12,21]. PB polymers with fcc structures are produced from hexacyanidoferrates complexes. The substitution of one CN^- to N-heterocycles ligands as isn (pyridine-4-carboxylate)[21], mpz (N-methylpyrazinium)[12] and ppt (5-(4-pyridil)-1H-1,2,4-triazole-3-thiol)[11] promotes loss of symmetry and crystallinity of the polymers. Thus, the higher electroactive area of SPE/PB-Ammine produced can be associated to its structural defects. On the contrary, the PB-Ammine-SPE presents the lower electroactive area, due to its decreased dispersibility in the carbonaceous matrix compared to the PB-SPE.

According to Table 1, the modified electrodes produced by the drop-casting method present larger electroactive areas, because of higher amount of the PB and PB-Ammine utilized and it reflects in the heterogeneous rate constants (k^0). The increase of the peak-to-peak separation in the voltammograms (Table S.9) indicates the slower electron transfer after the modification of the electrodes. The ferric cyanidoferrates polymers have partially blocked the interfacial charge transfer of the redox probe. The faster heterogenous electron transfer from the redox probe to the PB-Ammine-SPE is also atributed to the low dispersibility of this material and better exposure of the conductive carbon material used in the ink.

**Table 1:** Electroactive areas and heterogeneous rate constants of the SPEs

Electrode	Method	A_e (cm^2)	k^0 (cm s^{-1})
SPE		0.0718	1.91 x 10^{-3}
PB-SPE	ink*	0.0892	1.00 x 10^{-3}
PB-SPE-Ammine	ink*	0.0466	1.28 x 10^{-3}
SPE/PB	drop-casting	0.0829	1.02 x 10^{-3}
SPE/PB-Ammine	drop-casting	0.0992	0.23 x 10^{-3}

*incorporation of ECP into the ink

1 *3.2.Stabilities of the modified screen-printed electrodes at different pH*

2   The stabilities of the modified electrodes were investigated by cyclic voltammetry in 0.1 M ABS

3 (pH 6.0) containing 0.1 M KCl and in 0.1 M HCl/KCl (pH 1.0), according to Figures S.7-10. The

4 percentages of PB or PB-Ammine film in function of the scan is showed in Figure 2. The lower stability

5 of the modified SPEs at pH 6.0 compared to pH 1.0 was as expected, due to the affinity of OH^- ions for

6 Fe(III) at pH close to 7.0, breaking the Fe^{2+}–(CN)–Fe^{3+} bond [22].
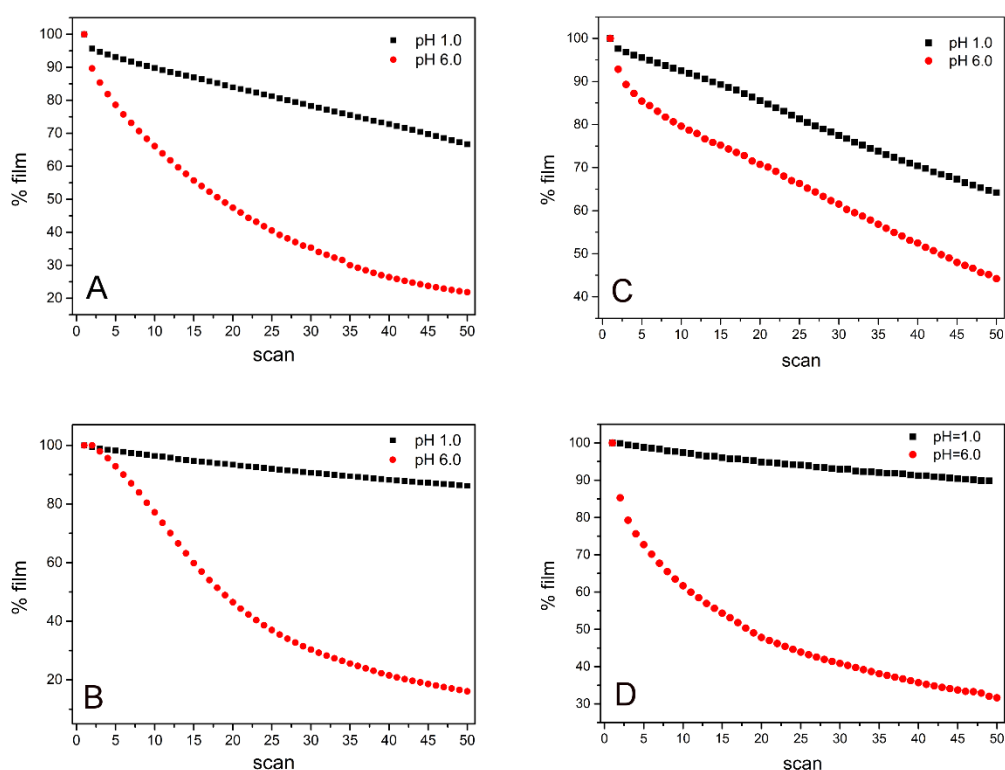
8 **Figure 2:** Comparison between the percentages of films in function of the number of scans at pH 1.0
9 and 6.0 of the modified electrodes: *incorporation of ECP into the ink*: **A)** PB-SPE, **B)** PB-Ammine-SPE,
10 *drop-casting:* **C)** SPE/PB and **D)** SPE/PB-Ammine.

12   It is well known that the stability of the ferric hexacyanidoferrates polymers can be increased by

13 electrochemical and thermal activations. These processes decrease the structural defects caused by the

14 coordination of OH^- to Fe^{3+} during the formation of PB or PB-Ammine and remove water present within

15 the crystals. However, the lability of the NH_3 ligand favours the exchange to H_2O or OH^- [23] at pH 6.0,

16 affecting the structure of the SPEs modified with PB-Ammine and explains their lower stabilities.

1   The stability of the ferric cyanidoferrates polymers is also dependent on the method of deposition,

2   due to the difference in availability of the ferric ions which can react with OH⁻. In addition, the "soluble"

3   form of PB is reported as the most stable one. From electrochemical activation, the "insoluble" form of

4   Prussian can be converted in to "soluble" form by insertion of K^+ in the interstitial sites[24]. However,

5   only the superficial layers of PB are able to be converted, due to direct contact with the KCl solution[19].

6   It can explain the higher stability and more effective activation of the modified SPEs by drop-casting

7   than the modification with the ink. In the other method, PB and PB-Ammine crystals are in the bulk of

8   the electrode, entrapped in the carbonaceous matrix, presented as "insoluble" form.

9

10   *3.3.Electrocatalytic properties*

11   To determine the effect of pH on the electro-oxidation of cysteine at the bare SPE, cyclic

12   voltammetry experiments at different pH in the presence of the analyte were performed (Figure S.11).

13   The electrochemical oxidation of cysteine (RSH) to dissulfide cystine (RSSR) on the bare SPE surface

14   is proceed by Eq.5-7:

15 $$RSH \rightarrow RS^- + H^+ \qquad (5)$$

16 $$RS^- \rightarrow RS \bullet + e^- \qquad (6)$$

17 $$2RS \bullet \rightarrow RSSR \qquad (7)$$

18   As it can be seen in Figure 3, the peak current increases with the pH. At higher pH deprotonation

19   of RSH (pKa = 8.37) occurs producing RS⁻, which is oxidized to RSSR *via* formation of sulfide

20   radical[25], explaining the better response at pH 6.0. The lower peak potential at pH 6.0 is also explained

21   as function of the deprotonation of cysteine. According to Fei and co-authors, at alkaline medium, the

22   oxidation peak shifts to more cathodic potentials[26]. However, detection of cysteine in alkaline solution

23   affects the stability of the ferric cyanidoferrates polymers. In our previous report, it was demonstrated

24   that acetate buffer solution is the best choice for electrochemical experiments using modified electrodes

1   with PB and analogues coordination polymers, causing small alterations in its structure[12]. In this sense,

2   pH 6.0 is more appropriate for cysteine detection.
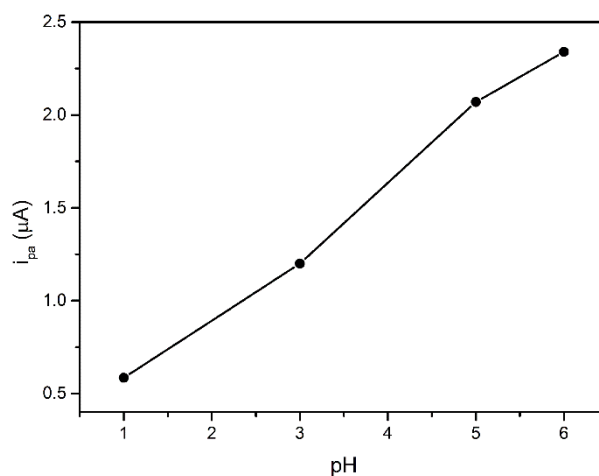
3

4   **Figure 3:** Plot of peak current of cysteine electro-oxidation at the bare SPE *versus* pH, in 1 mM cysteine
5   and 0.1 M KCl/HCl (pH 1.0) or 0.1 M ABS/KCl (pH 3.0, 5.0 and 6.0), at 5 mV s^{-1}.

6

7   The electro-oxidation of cysteine at the bare and modified SPEs was compared by cyclic

8   voltammetry at the chosen pH. Upon addition of cysteine, a pronounced increase of the current density

9   was observed for the modified SPEs, due to the electrocatalytic activity of the PB and PB-Ammine

10   toward the oxidation of the analyte, Figure 4 .
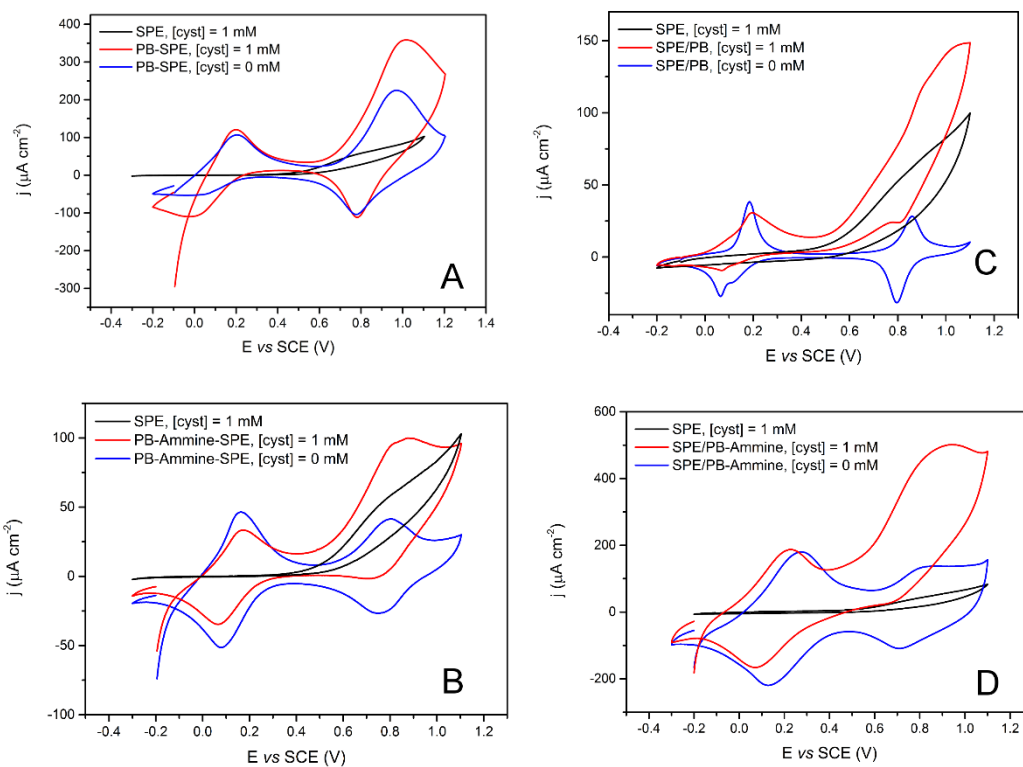
Figure 4: Comparison between the cyclic voltammograms of the bare SPE and modified: **A)** PB-SPE, **B)** PB-Ammine-SPE, **C)** SPE/PB and **D)** SPE/PB-Ammine in the absence and presence of 1 mM of cysteine. All the measurements were performed in 0.1 M ABS (pH = 6.0) and 0.1 M KCl at 5 mV s^{-1}.

For better understanding of the electro-catalytic oxidation of cysteine on the surface of the modified SPEs, cyclic voltammetry experiments at different scan rates in presence of 1.0 mM of this analyte were performed, Figure 5.
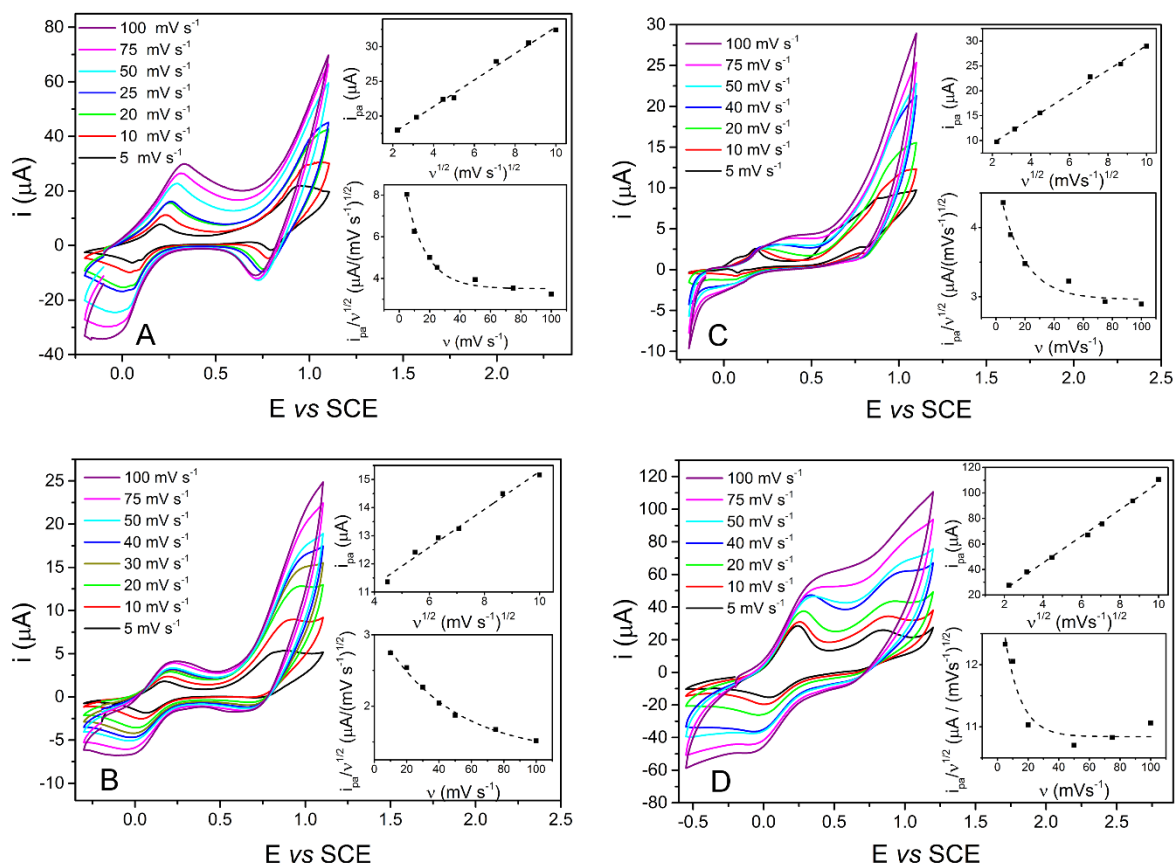
Figure 5: Cyclic voltammograms of **A)** PB-SPE, **B)** PB-Ammine-SPE, **C)** SPE/PB and **D)** SPE/PB-Ammine in presence of 1.0 mmol L^{-1} at various scan rates. All studies were performed in 0.1 M ABS (pH = 6.0) and 0.1 M KCl. Insert: plot of i_{pa} *versus* $\nu^{1/2}$ and plot of $i_{pa}/\nu^{1/2}$ *versus* ν.

The catalytic oxidation peak current (i_{pa}) increases linearly in function of the square root of the scan rate ($\nu^{1/2}$) in all modified electrodes, indicating that the electro-catalytic processes are controlled by diffusion of cysteine at the studied scan rate range in all modified electrodes, as can be expressed by Eq. 8-11 for the PB-SPE (ink), PB-Ammine-SPE (ink), SPE/PB (drop-casting) and SPE/PB-Ammine (drop-casting), respectively. In addition, characteristic shapes of a catalytic electrochemical process (EC$_{cat}$) were observed by plotting the scan rate normalized current ($i_{pa}/\nu^{1/2}$) *versus* scan rate, confirming the electro-catalytic efficiency of the ferric cyanidoferrate polymers.

$$I(\mu A) = 13.7 + 1.9\, \nu^{\frac{1}{2}}(mV\ s^{-1})^{\frac{1}{2}} \qquad (8)$$

$$I(\mu A) = 8.5 + 0.7\, \nu^{\frac{1}{2}}(mV\ s^{-1})^{\frac{1}{2}} \qquad (9)$$

1 $$I(\mu A) = 4.5 + 2.5\ v^{\frac{1}{2}}(mV\ s^{-1})^{\frac{1}{2}} \qquad (10)$$

2 $$I(\mu A) = 3.2 + 10.5\ v^{\frac{1}{2}}(mV\ s^{-1})^{\frac{1}{2}} \qquad (11)$$

3 Cysteine (RSH) can be electro-oxidized to dissulfide cysteine (RS-SR) by Fe^{3+} ions in the PB or

4 PB-Ammine structures, which is reduced to Fe^{2+}. The generic reaction for cysteine oxidation on the

5 surfaces of the modified SPEs has been proposed as follows:[27,28]

6 $$Fe^{3+} + 2RSH \xrightarrow{K_{obs}} Fe^{2+} + RS - SR + 2H^{+} \qquad (9)$$
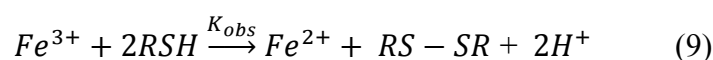
7 To compare the kinetic of the chemical reactions between the Fe^{3+} ions in the PB or PB-Ammine

8 modified SPEs and cysteine, chronoamperometric experiments in the presence of different

9 concentrations of the analyte were performed, Figure 6. The heterogeneous rate constants, k_{obs} of these

10 reactions were determined according to Eq. 10.

11 $$\frac{i_{cat}}{i_0} = \gamma^{\frac{1}{2}} \pi^{\frac{1}{2}} = \pi^{\frac{1}{2}}(k_{obs}Ct)^{\frac{1}{2}} \quad (10)$$

12 where i_{cat} is the catalytic current of the modified SPEs in the presence of cysteine, i_0 is the limiting

13 current in the absence of cysteine and $\gamma = k_{obs}Ct$ (C is the bulk concentration of cysteine and t is the

14 elapsed time)[29].
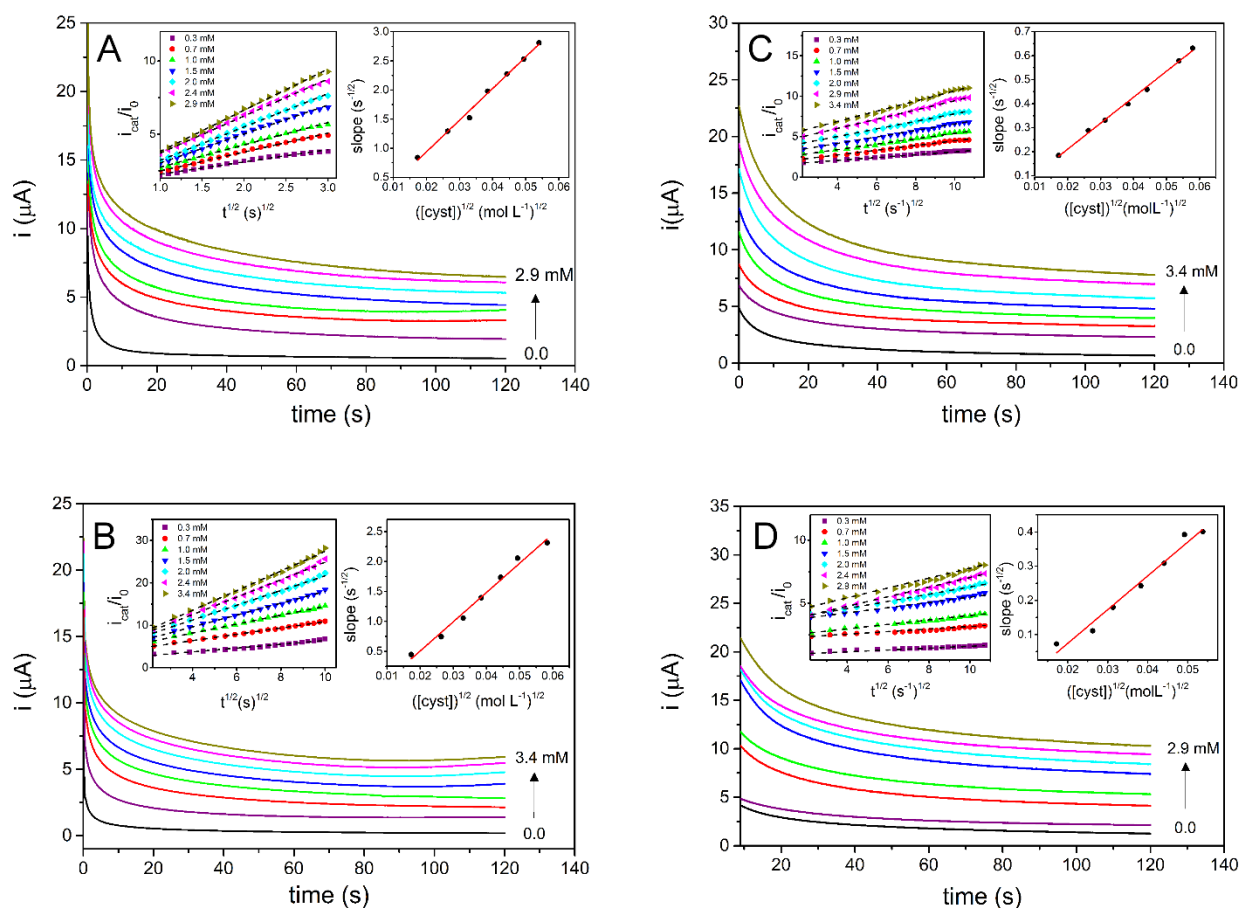
Figure 6: Chronoamperograms of **A)** PB-SPE, **B)** PB-Ammine-SPE, **C)** SPE/PB and **D)** SPE/PB-Ammine in 0.1 M ABS at pH 6.0 different concentrations of cysteine. Inserts: Curves of i_{cat}/i_0 *versus* $t^{1/2}$ for the same concentrations of cysteine, and plot of the slopes of these curves *versus* the square root of the concentrations of cysteine.

The heterogeneous rate constants were obtained from the linear plots of i_{cat}/i_0 *versus* $t^{1/2}$. Then, graphs of the slopes of these curves were plotted as a function of the square root of the concentrations of cysteine ($[cyst]^{1/2}$). Finally, k_{obs} were calculated from the slopes of these graphs, resulting in values of 9.4×10^2, 3.6×10^2, 3.7×10^1 and 3.1×10^1 L mol^{-1} s^{-1} for PB-SPE (ink), PB-Ammine-SPE(ink), SPE/PB (drop-casting) and SPE/PB-Ammine (drop-casting), respectively. The modified SPEs by the incorporation of the materials in the ink presents lower stability due to more exposure of the Fe^{3+}. However, the high availability of these sites increases the heterogeneous rate constants for cysteine electro-oxidation at PB-SPE and SPE-PB-Ammine. The faster kinetics of the chemical reactions

1 between the Fe^{3+} ions in the PB-SPE and cysteine is attributed to the better distribution of this material

2 and its higher electroactive area. To compare the performances of the modified electrodes for sensing of

3 cysteine, chronoamperometric experiments were carried out.

4 *3.4.Chronoamperometric detection of cysteine*

5   Aiming cysteine detection, Figure 7 displays the choronoamperometric responses of bare SPE,

6 SPE/PB (drop-casting), SPE/PB-Ammine (drop-casting), PB-SPE (ink) and PB-SPE-Ammine (ink)

7 after successive additions of cysteine in 0.1 mol L^{-1} ABS and 0.1 mol L^{-1} KCl at pH 6.0. As it can be

8 seen in Figure S.12, with an applied potential of 0.8 V *vs* SCE, the SPEs showed linear responses in the

9 ranges presented in Table 2.
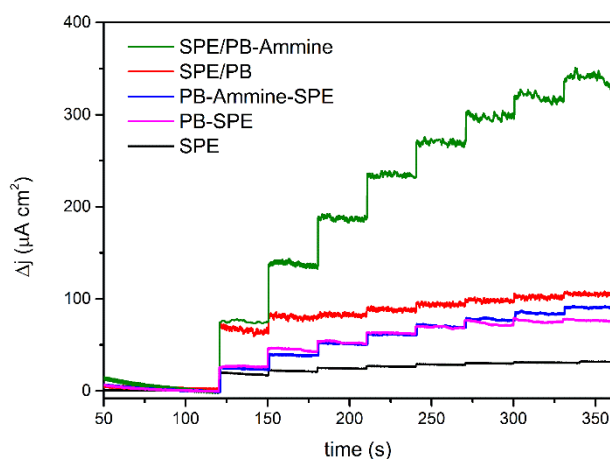
10

11 **Figure 7:** Chronoamperograms of the bare and modified SPEs: PB-SPE, PB-Ammine-SPE, SPE/PB and
12 SPE/PB-Ammine in 0.1 M ABS at pH 6.0 and 0.1 M KCl after successive additions of 0.1 mol L^{-1}
13 cysteine. Applied potential of 0.8 V *vs* SCE.

14 **Table 2:** Comparison of the amperometric responses of the modified electrodes

Electrode	Linear dependence	R^2	Linear range	LOD
*PB-SPE	$\Delta i(\mu A) = 7.03 \times 10^{-3}$ [cyst]$(\mu M) + 2.80$	0.99	200-600 μM	45.1 μM
*PB-Ammine-SPE	$\Delta i(\mu A) = 3.61 \times 10^{-3}$ [cyst]$(\mu M) + 1.58$	0.99	300-800 μM	102.4 μM
†SPE/PB	$\Delta i(\mu A) = 4.24 \times 10^{-3}$ [cyst]$(\mu M) + 5.55$	0.99	300-700 μM	70.2 μM
†SPE/PB-Ammine	$\Delta i(\mu A) = 4.89 \times 10^{-2}$ [cyst]$(\mu M) + 3.58$	0.99	100-500 μM	58.6 μM

15 *incorporation of ECP into the ink;* †drop-casting

1 The electro-oxidation of cysteine at the surface of the modified SPEs begins with the

2 deprotonation of this molecule, which is diffused from the bulk solution to the electrode surface. On the

3 PB or PB-Ammine modified SPE surface, the deprotonated cysteine is oxidized by the Fe^{3+} ions in the

4 PB or PB-Ammine in an electro-catalytic process. The performances of the electrodes towards detection

5 of cysteine are dependent on the stabilities of the electrodes, the electron transfer from the modified

6 electrode to the analyte, the availability of the ferric ions and the kinetics of the chemical reaction

7 between the catalytic sites and the analyte. Comparing the different ferric cyanidoferrates and the

8 modification methods, the lower detection limit was obtained at the PB-SPE, due to its high electroactive

9 area and availability of Fe^{3+} catalytic sites. In addition, the incorporation of a non-conductive material

10 as PB in the ink allows a less pronounced decrease of the heterogeneous electron transfer rate than the

11 drop-casting method. Although PB-ammine electrochemical potentials are shifted to lower values than

12 PB, the PB-ammine transfer rate is lower than PB (see Figure S.13). This feature can explain the

13 differences observed in the oxidation of cysteine (k_{obs}) and in the sensing of this analyte.

14

15 **4. Conclusion**

16 Ferric cyanidoferrates polymers, PB and PB-Ammine, synthesized from different monomers

17 $[Fe(CN)_6]^{4-}$ and $[Fe(CN)_5NH_3]^{3-}$ were used to modify screen-printed electrodes. The modification was

18 performed by two methods, the drop-casting and the incorporation of the materials in the ink used in the

19 screen-printed process. The SPE modified by PB-Ammine (drop-casting) has the highest electroactive

20 area. However, the highest heterogeneous rate constants are found in SPE modified by PB-Ammine

21 incorporated into the ink. All of them have catalytic behaviour to electro-oxidation of cysteine, but the

22 highest value of k_{obs} and lowest limit of detection was observed in the SPE modified by PB incorporated

23 into the ink. These results suggest that the electrocatalytic properties of SPE modified by PB and PB-

24 Ammine are dependents of the availability of Fe^{3+} catalytic sites and the faster chemical reaction between

25 the catalytic sites and the analyte.

Conflict of interest

The authors declare that there is no conflict of interests regarding the publication of this study.

Acknowledgements

Supporting Information

Supporting Information associated with this article can be found in the online version.

References

[1]   C. W. Foster, R. O. Kadara, C. E. Banks, in *Screen-Print. Electrochem. Archit.*, Springer International Publishing, Cham, **2016**, pp. 1–23.

[2]   E. P. Randviir, D. A. C. Brownson, J. P. Metters, R. O. Kadara, C. E. Banks, *Phys. Chem. Chem. Phys.* **2014**, *16*, 4598.

[3]   J. R. Windmiller, J. Wang, *Electroanalysis* **2013**, *25*, 29–46.

[4]   F. E. Galdino, C. W. Foster, J. A. Bonacin, C. E. Banks, *Anal Methods* **2015**, *7*, 1208–1214.

[5]   N. Jadon, R. Jain, S. Sharma, K. Singh, *Talanta* **2016**, *161*, 894–916.

[6]   S. Sadeghi, A. Garmroodi, *Electroanalysis* **2013**, *25*, 323–330.

[7]   C. W. Foster, J. P. Metters, D. K. Kampouris, C. E. Banks, *Electroanalysis* **2014**, *26*, 262–274.

[8]   Y. Cui, *IEEE Trans. Electron Devices* **2017**, *64*, 2467–2477.

1 [9]   S. Shahrokhian, *Anal. Chem.* **2001**, *73*, 5972–5978.

2 [10] M. C. Gallo, B. M. Pires, K. C. F. Toledo, S. A. V. Jannuzzi, E. G. R. Arruda, A. L. B. Formiga, J.

3   A. Bonacin, *Synth. Met.* **2014**, *198*, 335–339.

4 [11] B. M. Pires, F. E. Galdino, J. A. Bonacin, *Inorganica Chim. Acta* **2017**, *466*, 166–173.

5 [12] M. C. Monteiro, K. C. F. Toledo, B. M. Pires, R. Wick, J. A. Bonacin, *Eur. J. Inorg. Chem.* **2017**,

6   DOI 10.1002/ejic.201601540.

7 [13] A. L. B. Formiga, S. Vancoillie, K. Pierloot, *Inorg. Chem.* **2013**, *52*, 10653–10663.

8 [14] E. Blanco, C. W. Foster, L. R. Cumba, D. R. do Carmo, C. E. Banks, *The Analyst* **2016**, *141*, 2783–

9   2790.

10 [15] S. J. Rowley-Neale, G. C. Smith, C. E. Banks, *ACS Appl. Mater. Interfaces* **2017**, *9*, 22539–22548.

11 [16] I. Lavagnini, R. Antiochia, F. Magno, *Electroanalysis* **2004**, *16*, 505–506.

12 [17] J. P. Metters, R. O. Kadara, C. E. Banks, *The Analyst* **2011**, *136*, 1067.

13 [18] L. R. Cumba, C. W. Foster, D. A. C. Brownson, J. P. Smith, J. Iniesta, B. Thakur, D. R. do Carmo,

14   C. E. Banks, *The Analyst* **2016**, *141*, 2791–2799.

15 [19] F. Ricci, G. Palleschi, *Biosens. Bioelectron.* **2005**, *21*, 389–407.

16 [20] K. Itaya, I. Uchida, V. D. Neff, *Acc. Chem. Res.* **1986**, *19*, 162–168.

17 [21] B. Morandi Pires, S. A. Venturinelli Jannuzzi, A. L. Barboza Formiga, J. Alves Bonacin, *Eur. J.*

18   *Inorg. Chem.* **2014**, *2014*, 5812-N5819.

19 [22] A. Karyakin, *Electrochem. Commun.* **1999**, *1*, 78–82.

20 [23] N. Ghasdian, Y. Liu, R. McHale, J. He, Y. Miao, X. Wang, *J. Inorg. Organomet. Polym. Mater.*

21   **2013**, *23*, 111–118.

22 [24] R. J. Mortimer, D. R. Rosseinsky, *J. Chem. Soc. Dalton Trans.* **1984**, 2059.

23 [25] W. T. Tan, A. M. Bond, S. W. Ngooi, E. B. Lim, J. K. Goh, *Anal. Chim. Acta* **2003**, *491*, 181–191.

24 [26] S. Fei, J. Chen, S. Yao, G. Deng, D. He, Y. Kuang, *Anal. Biochem.* **2005**, *339*, 29–35.

25 [27] C. C. Corrêa, S. A. V. Jannuzzi, M. Santhiago, R. A. Timm, A. L. B. Formiga, L. T. Kubota,

26   *Electrochimica Acta* **2013**, *113*, 332–339.

27 [28] N. Hernández-Ibáñez, I. Sanjuán, M. Á. Montiel, C. W. Foster, C. E. Banks, J. Iniesta, *J.*

28   *Electroanal. Chem.* **2016**, *780*, 303–310.

29 [29] J.-B. Raoof, R. Ojani, H. Beitollahi, *Electroanalysis* **2007**, *19*, 1822–1830.

30